Membrane Fluctuation Model for Understanding the Effect of Receptor Nanoclustering on the Activation of Natural Killer Cells through Biomechanical Feedback

Ashish Pandey,[†,‖] Piotr Nowakowski,[‡,‖] Carlos Ureña Martin,[†] Muhammad Abu Ahmad,[¶] Avishay Edri,[¶] Esti Toledo,[†] Sivan Tzadka,[†] Jonas Walther,[§] Guillaume Le Saux,[†] Angel Porgador,[¶] Ana-Sunčana Smith,[*,§,‡] and Mark Schvartzman[*,†]

†*Department of Materials Engineering, Ben-Gurion University of the Negev, P.O. Box 653, Beer-Sheva 84105, Israel; Ilse Katz Institute for Nanoscale Science and Technology, Ben-Gurion University of the Negev P.O. Box 653, Beer-Sheva 84105, Israel*

‡*Group for Computational Life Sciences, Division of Physical Chemistry, Ruđer Bošković Institute, Bijenička 54, 10000, Zagreb, Croatia*

¶*The Shraga Segal Department of Microbiology, Immunology, and Genetics, Faculty of Health Sciences, Ben-Gurion University of the Negev, P.O. Box 653, Beer-Sheva 84105, Israel*

§*PULS Group, Institut für Theoretische Physik, IZNF, Friedrich-Alexander-Universität Erlangen-Nürnberg, Cauerstraße 3, 91058 Erlangen, Germany*

‖*These authors contributed equally.*

E-mail: smith@physik.fau.de,asmith@irb.hr; marksc@bgu.ac.il

Abstract

We investigated the role of ligand clustering and density in the activation of natural killer (NK) cells. To that end, we designed reductionist arrays of nanopatterned ligands arranged with different cluster geometries and densities, and probed their effects on NK cell activation. We used these arrays as an artificial microenvironment for the stimulation of NK cells, and studied the effect of the array geometry on the NK cell immune response. We found that ligand density significantly regulated NK cell activation, while ligand clustering only had an impact at a specific density threshold. We also rationalized these findings by introducing a theoretical membrane fluctuation model that consider biomechanical feedback between ligand–receptor bonds and the cell membrane. These findings provide an important insight into NK cell mechanobiology, which is fundamentally important and essential for designing immunotherapeutic strategies targeting cancer.

Keywords

natural killer cells, nanolithography, activation, clustering, immune response

Natural killer (NK) cells are the sentinels of our innate immune system and are nowadays extensively studied due to their growing use in immunotherapy,[1,2] including effective cancer treatments.[3,4] NK cells recognize pathogens, viral and tumor cells using receptors that specifically bind ligands expressed by their targets.[5] The binding of these receptors initiate cascades of activating, costimulatory, and inhibitory signals, the balance of which determines whether the target cell will be tolerated or killed by either cytotoxic or lytic mechanism.[6–8]

Activation of NK cells, as well as other lymphocytes such as T cells, involves the formation of nanometric clusters of receptors[9–13] that stabilize the contact between the membrane of the lymphocyte and the target cell, using membrane-mediated and direct interactions. Clusters, furthermore, facilitate the spatial exclusion of large phosphatases. The kinase–phosphatase balance is thus shifted at the receptor cytodomain towards the phosphatase causing lymphocyte activation.[14] Such exclusion by size promotes equally sized ligand–receptor constructs

to group within a small confinement, further promoting clustering and increasing the number of formed bonds.[15,16]

The relation between the ligand spatial arrangement and the lymphocyte activation was studied using surfaces with controlled ligand positioning. Arrays functionalized with antibodies or their binding fragments were employed to study the activation of T cells,[17–19] where the ∼10 nm nanodot size ensures that about one ligand, on average, occupies single nanodot, ensuring molecular scale control of the receptor arrangement.[20] However, antibodies do not precisely mimic the kinetics of physiological ligand–receptor interaction since the affinity of the receptor for the antibody is a few orders of magnitude higher than that for the ligand. Utilizing the fact that, unlike T cells, NK cells are not antigen-specific we studied the role of the spatial arrangement of activating ligands in the activation of NK cells, using nanolithographically patterned periodic arrays of ∼10 nm metallic nanodots functionalized with activating ligands for NK cells.[21] In particular, we found that the activation of NK cell increased upon increasing the density of ligands, reaching the activation saturation at the threshold density of ∼100 ligands/μm^2. Furthermore, we later engineered more sophisticated arrays presenting controllably spaced activating and inhibitory ligands for NK cells, and demonstrated that this spacing regulates the inhibition of NK cell activation and signaling.[22] Thereby, we showed that the interplay between the membrane dynamics and the bio-mechanical properties of activating and inhibitory ligand–receptor constructs determine the fate of the target cell.

Another indicative finding is that the activation of cells can be associated with changes in the state of the cell membrane, evidenced by the appearance of strong shape fluctuations on the cell surface.[23–27] The increase of membrane fluctuations caused by functional activity has been reported for all cell types in which this was measured, including red blood cells, macrophages,[23] HeLa cells, epithelial CHO, C2C12, myoblasts,[26] T-lymphocytes,[25] fibroblasts,[28] and others. The reason for this relation lies in the low bending stiffness of the membrane, which makes membrane fluctuations directly coupled to fast cytoplasmic actin re-

structuring, cytoplasmic flows, and intensive membrane trafficking. All these processes play a role in NK cell activation. For example, actin flows intensify in activated NK cells.[29] Similarly, NKG2D receptor activation induces downstream actin reorganization through DAP10, Grb2 and, ultimately, VAV1 proteins.[30] NKG2D activation also relates to the elevation of intracellular calcium,[30] which involves an increase of membrane transport. Furthermore, enhanced dynamics was found in IL-2-activated cells.[31] Another relevant example highlighting the importance of membrane fluctuations comes from an explicit demonstration that the target membrane dynamics determines the NK cell killing mechanisms.[32] Finally, membrane dynamics was found to be crucial for the regulation of NKG2D promoted activation,[22] pointing to a relation between the membrane and the ligand–receptor complexation rates.

Actually, binding and unbinding rates are established determinants of signaling. It was experimentally suggested[13,16] and theoretically demonstrated[33] that one receptor more readily binds and rebinds its cognate ligand in the vicinity of another already-formed ligand–receptor construct. This is induced by membrane-mediated cooperativity that provides effectively larger affinity of ligand–receptor bonds building the cluster, as compared to lone bonds.[33,34] The high on–off rate of the receptor–ligand binding, in turn, can produce the engagement of multiple receptors by one ligand, which makes even one individual ligand enough to induce substantial activating signaling.[35] Furthermore, the intensification of membrane fluctuations in activated cells was found to increase binding and unbinding rates, as well as the effective binding affinity of the pair.[36] It is therefore expected that the state of the membrane couples to receptor clustering.

The research clearly points to a relation between the state of the cell during activation by the engagement of activating receptors, the change in the state of the membrane, captured by the intensity of its fluctuations, the receptor binding, and the formation of domains. Nevertheless, it is unknown whether the formation of receptor domains is a mandatory precondition or consequence of signaling and the ensuing activation. By establishing a membrane fluctuation model (MFM), we hypothesize that the fluctuation-induced coupling between

receptor–ligand constructs acts as a biomechanical feedback loop in the control of activation through the state of the membrane, a possibility that has not yet been considered.

To separate the effect of bond organization and density, as well as to explore the existence of the mechanical feedback, we designed reductionist arrays with ligation sites arranged in distinct clusters and varied their size (*i.e.* number of sites per cluster). We focused on the effect of the nanoscale arrangement of MICA ligands that engage NKG2D receptors. Given that other receptors provide only a limited synergy with NKG2D or are highly dependent on the signaling of costimulatory receptors,[37,38] and that adding ligands for these receptors would likely produce a screening effect on the role of the MICA arrangement, other receptors, like 2B4 or LFA-1, were excluded from the study. Consequently, we produced arrays with three global MICA densities at which the clusters are organized—one associated with the previously reported threshold, one below, and one above it. We stimulated primary NK cells on these arrays, and confirmed that the density (hence, the number of formed bonds) is a major regulator of NK cell activation. Ligand clustering correlated with the activation only for the threshold density, otherwise having no effect. We develop our MFM to show that these results can be explained by considering the biomechanical feedback provided by the membrane. Below the threshold density, number of formed bonds is not sufficient to change the state of the membrane, and clustering plays no role. High above the threshold, so many bonds are formed that the signal is saturated, regardless of the cluster size. Around the threshold, membrane mediated correlations play a role, which demonstrates the importance of cell biomechanics in the regulation of activation.

The most precise way to arrange the ligands is by their tethering to nanofabricated arrays of nanodots.[39,40] We fabricated the nanodot arrays on Si wafers using electron beam lithography, Au evaporation, and liftoff (Fig. 1). The nanodots are functionalized with his-tagged MHC class I polypeptide-related sequence A (MICA)—a ligand that binds NKG2D[41]—attaching to a monolayer of thiols terminated with nitrilotriacetic acid (NTA).[42] The silicon background was coated with Poly-L-lysine (PLL) to facilitate cell adhesion (see the Sup-

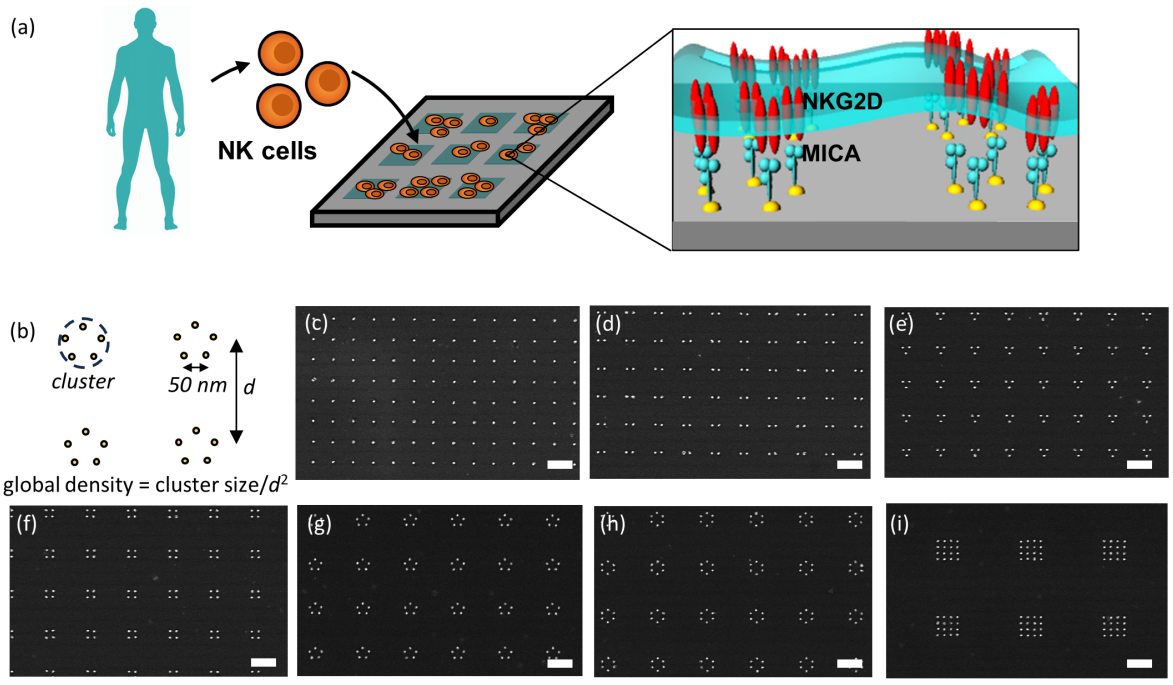

Figure 1: Establishing a mimetic system to study the activation of NK cells. (a) Scheme of NK cell stimulation on a pattern of ligand clusters. (b) Schematic plot of the patterns used in the experiment. The distance between neighboring nanodots within one cluster is 50 nm. Clusters form a square lattice with a lattice constant d chosen such that overall density of nanodots is 40, 100, or 250 dots/µm^2. (c)–(i) SEM images of nanoarray containing different arrangement of nanodots: (c) single dot, (d) two dots, (e) triangle, (f) square, (g) pentagon, (h) hexagon, and (i) cluster of 16 dots. On each of the presented images the density is 40 dots/µm^2 and scale bar is 200 nm long.

porting Information (SI) for details of the fabrication and biofunctionalization process). For the nanodot size of ∼10 nm, on average around one ligand was found to tethered to each nanodot,[20] ensuring molecular level control of the receptor positioning.

We designed arrays with various clusters, containing from one nanodot up to 16 ligated nanodots (Fig. 1(c)–(i)). The chosen range of sizes and distributions of the clusters is based upon the nanoscale clusters formed between MICA ligands and NKG2D receptors microscopically observed on the NK cell–target interface.[43] We used three global densities: 40, 100, and 250 nanodots/µm^2, by tuning the spacing between the clusters in each case. Notably, the global density of 100 nanodots/µm^2 corresponds to previously found threshold activation density in continuous arrays,[21] while the densities of 40 nanodots/µm^2 and

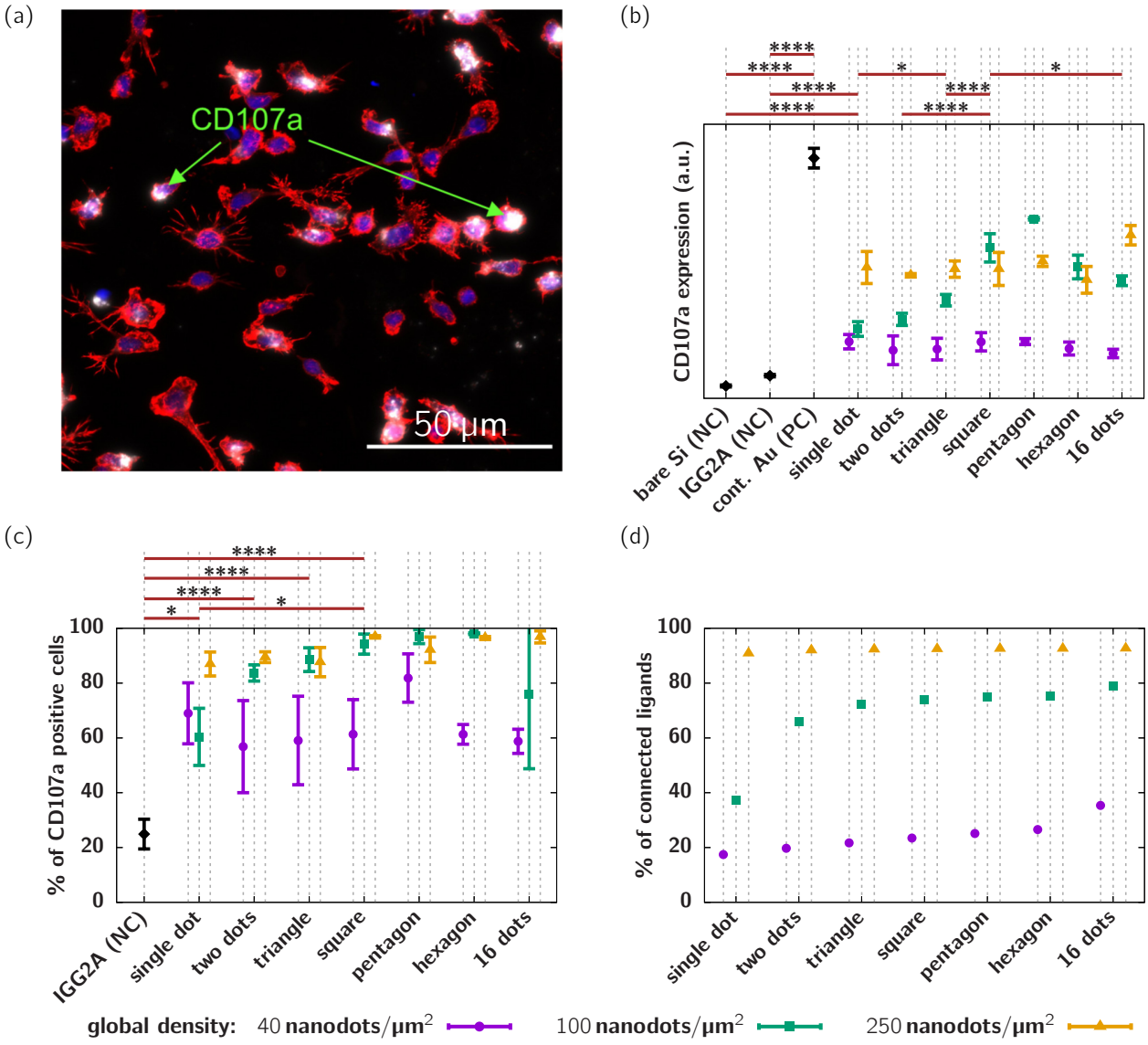

Figure 2: Effect of patterning on the activation of NK cells. (a) Representative image of activated NK cells on ligand-functionalized surfaces. Cells were stained with phalloidin for cytoskeleton (red), DAPI for nuclei (blue) and CD107a (white). Panels (b) and (c) present the plots of CD107a expression quantified by measuring the fluorescence intensity of the APC-labeled anti-CD107a, and percentage of CD107a positive cells, respectively. Each measurement has been done for seven different sizes of the clusters (as denoted on horizontal axes) and for three different overall densities of ligands (denoted by color—violet for 40, green for 100, and orange for 250 ligands/µm^2). The study was conducted using triplicates in each data set. On average, approximately 80–100 cells per data set in each singlet were taken. Eight fields of view were taken to achieve a quantifiable number of cells in each set. The pictograms above the graphs show statistical significance of differences for selected pairs, calculated with Tukey's multiple-comparison tests using the GraphPad Prism software. $*\,p < 0.05$, $**\,p < 0.01$, $***\,p < 0.001$, $****\,p < 0.0001$. Full data for the statistical significance is presented in Supporting Information in Tables S1 and S2. (d) Percentage of bound ligands calculated from our theoretical model.

250 nanodots/μm^2 correspond to continuous arrays for insufficient and saturated activation, respectively. Additionally, we used three types of controls: (*i*) Bare Si coated with PLL, (*ii*) Si/Au functionalized with a continuous layer of non-specific IGG2A as a negative controls, and (*iii*) Si/Au functionalized with a continuous layer of MICA as a positive control.

We isolated primary NK cells from peripheral blood mononuclear cells of a healthy donor, stimulated them on the fabricated arrays, and studied their cytotoxic response as a function of the array geometry. As the benchmark of cytotoxicity, we imaged Lysosomal-associated membrane protein 1 (LAMP1), also called CD107a. During the activation of NK cells, CD107a is released from lytic granules together with granzymes and perforin, and expressed on the cell surface, which makes CD107a a broadly used activation marker for NK cells.[22,44] Here, we incubated the cells with APC-tagged antibody for CD107a for three hours, fixed them, stained the cytoskeleton and the nucleus with phalloidin and DAPI, respectively, and imaged them using a confocal microscope (white signal, Figure 2(a)).

To characterize the sensitivity of NK cell activation to the formation of clusters, we evaluate the average signal of CD107a per cell for all the probed global densities and cluster sizes (Figure 2(b)). Furthermore we quantify the percentage of CD107a-positive cells (cells expressing more CD107a than the average CD107a signal obtained on the negative control) to emphasize the effect of the array geometry on NK cell activation (Fig. 2(c)). We clearly see that the global density substantially affects CD107a expression, but the effect of cluster size is insignificant with 40 and 250 nanodots/μm^2. On the contrary, for 100 nanodots/μm^2 the activation increases upon increasing cluster size, until it reaches saturation at the clusters of four dots.

As expected, both negative controls (Si and IGG2A-coated surfaces) induced very low activation of NK cells. The positive control (MICA-functionalized continuous Au) produced activation even higher than the saturation level for patterned ligands. This ultra-high activity is a consequence of the several orders of magnitude higher density of bound receptors for continuous Au than for our patterned nanoarrays.[21]

Taken together, these data suggest that: (*i*) For the relatively low global density of ligands, which is significantly below the activation threshold of $\sim$100 ligands/µm^2, the activation is very low due to the insufficient total amount of the ligands available for the cells, regardless of the way the ligands are clustered. (*ii*) For the very high global density of ligands, which is way above the same activation threshold, the activation is very high, regardless of the way the ligands are clustered. This activation is comparable to that produced by arrays of closely packed ligands (positive control), suggesting that the trend of activation vs. ligand density eventually saturates. (*iii*) For the intermediate global density, around the activation threshold, for evenly distributed ligands their overall amount is too small to produce a significant activation of NK cells. However, this insufficient amount can be compensated by grouping the ligands into dense clusters, among which the cluster of four ligands seems to be around the threshold cluster size for the activation saturation, at least for the probed global density of 100 ligands/µm^2.

To rationalize these results, we construct a bottom–up theoretical Membrane Fluctuation Model (MFM) for NK cell activation, following the approach that successfully explained the inhibition of NKG2D signaling in NK cells.[22] MFM assumes a linear relation between the measured expression of CD107a and the density $\mathcal{N}$ of ligand–receptor bonds of the cell. In the stationary state, this density is given by $\mathcal{N} = \varrho\,\bar{K}_{\mathrm{on}}/\left(\bar{K}_{\mathrm{off}} + \bar{K}_{\mathrm{on}}\right)$, where ϱ is the density of ligands, and $\bar{K}_{\mathrm{on}}$ and $\bar{K}_{\mathrm{off}}$ denote the average binding and unbinding rates of ligand–receptor pairs within the cluster.

Because the receptors are embedded into the NK cell surface, the binding and unbinding rates are directly affected by the membrane fluctuation amplitude σ and the average position of the membrane h relative to the patterned surface. When the state of the membrane before binding is set (by σ and h), $\bar{K}_{\mathrm{on}}$ and $\bar{K}_{\mathrm{off}}$ can be calculated explicitly from first principles (see SI for details). The assumption here is that the ligand–receptor construct can be represented by a spring with stiffness λ and rest length l_0, and that each bond has an intrinsic affinity ε_{b}. In such a model, it was already shown that the binding rate of an individual bond increases

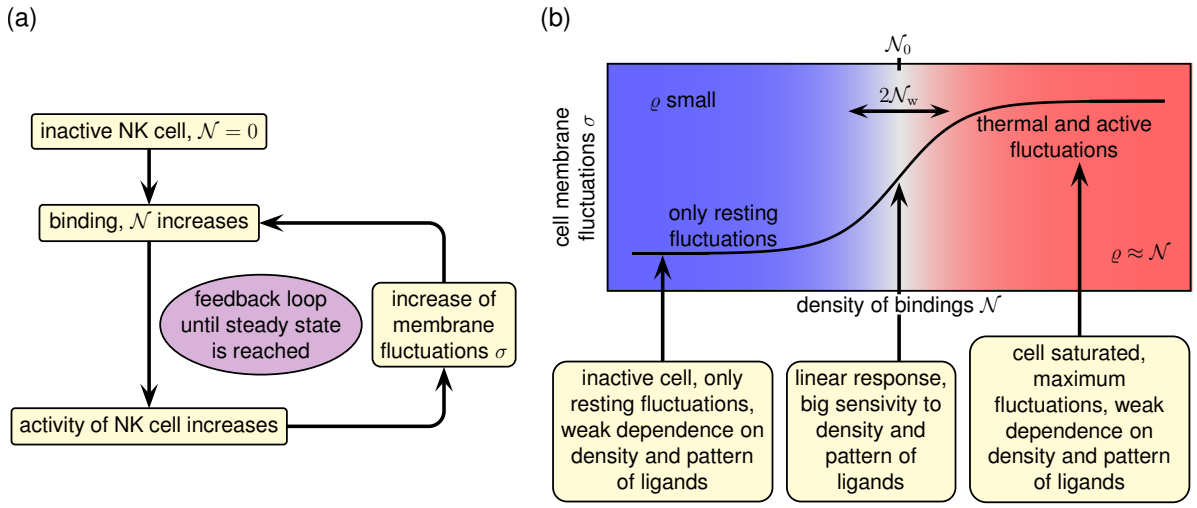

Figure 3: The membrane fluctuation model (MFM). (a) Schematic diagram shows the processes forming the feedback loop postulated in the MFM, leading to an enhancement of the activity of natural killer cell. (b) Sigmoid shape of the relation between membrane fluctuations σ and the density of ligand–receptor bonds $\mathcal{N}$. For small densities of ligands cell stays inactive and for large densities it is fully active, regardless of grouping of ligands. Only in the vicinity of the threshold density $\mathcal{N}_0$, the small increase in cell activity due to the grouping of ligands is enhanced by the feedback loop mechanism resulting in a strong dependence of activity on the size of the clusters of ligands.

dramatically upon activation of an immune cell, while the unbinding rate is also enhanced but to a lesser extent. Hence, the affinity grows significantly, and with it, the density of such (non-interacting) bonds.[36] Clustering, furthermore introduces correlations between bonds that are within the membrane lateral correlation length.[15,22] This is also reflected in the rates and the effective affinity, which are calculated in the SI for the patterns presented in Fig. 1.

Motivated by the measured logistic relation between bond density and cell activity, we introduce another important component of MFM—the mechano-signaling feedback loop (Fig. 3). Accordingly, forming of the bonds increases the activity of the cell; this proportionally increases the active fluctuations of the membrane (σ_{active}); which in turn, affects the rates in a non-linear fashion and promotes the creation of further bindings; ultimately amplifying the response of the cell. In agreement with experiments,[21,45] we assume that the dependence of σ_{active} on density of bonds $\mathcal{N}$ is sigmoid, which splits the behavior of the sys-

tem into three distinct regimes: for low densities of bonds (blue region in Fig. 3(b)) there is practically no activation, for moderate densities the enhancement via the mechano-signaling feedback loop can take place, and for high densities (red region in Fig. 3(b)) the activity only slowly growths as the density of bonds increases. The borders between these three regimes are defined by two parameters of the sigmoid curve: middle point $\mathcal{N}_0$ and thickness $\mathcal{N}_\mathrm{w}$ of the moderate densities region.

The model clearly shows (Fig. 2(d)) that at low densities of ligands, the number of formed bonds remains insufficient to induce activation. Grouping ligands into clusters slightly increases binding stability within the cluster ($\bar{K}_\mathrm{on}/\left(\bar{K}_\mathrm{off}+\bar{K}_\mathrm{on}\right)$ increases), but the low density of ligands sustains $\mathcal{N}$ insufficient to trigger the feedback and activate the NK cell. This is consistent with the insensitivity of the data to the patterning at low density.

Around the threshold density, the increase in $\bar{K}_\mathrm{on}/\left(\bar{K}_\mathrm{off}+\bar{K}_\mathrm{on}\right)$ due to stabilization of binding by clustering becomes sufficient to trigger the feedback mechanism: the activity of NK cell increases active cell fluctuations of the membrane and promotes further binding.

Finally, above the threshold density, the number of ligands is big enough to pull the membrane closer to the substrate and make practically all ligands bound to receptors. The density of bounds is so high that the effect of clustering on the rates diminishes and the number of formed bonds depends only on the density, in a linear fashion. This also explains the stronger activation for the positive control compared to activation due to patterned ligands whose overall density is two orders of magnitude lower.

Such a behaviour is also systmematically seen in Figure 4, which compares the percentage of CD107a positive cell and the calculated percentage of bound ligands vs. the global density for each cluster size separately, further emphasizes the dominant effect of the global density on the ligand–receptor binding, and its correlation with the NK cell activation.

To assess whether the ligand distribution affects NK cell spreading, we measured the average cell diameter after three hours of stimulation (Fig. 5(a)). The control surfaces produced a relatively uniform distribution of the cell area within the tested cell population.

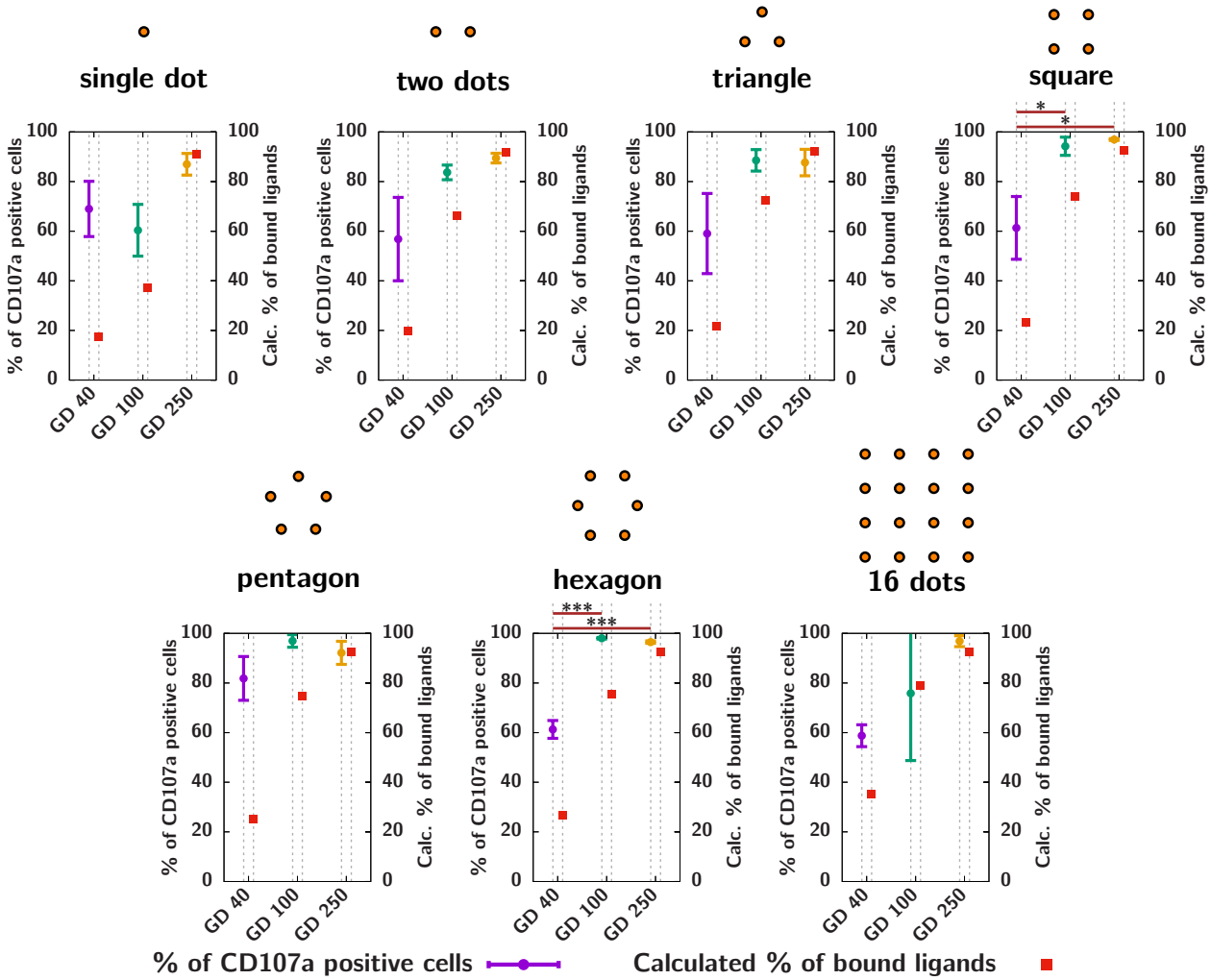

Figure 4: Comparison of measured percentage of CD107a positive cells with the calculated from our model percentage of bound ligands. Each panel presents the results for a different shape of the cluster of ligands, as schematically plotted above the graph. For every cluster the results for three different global densities (GD) are presented. The statistical significance of differences for some of the pairs of experimental points has been presented above the graphs using the same pictograms as on Figure 2.

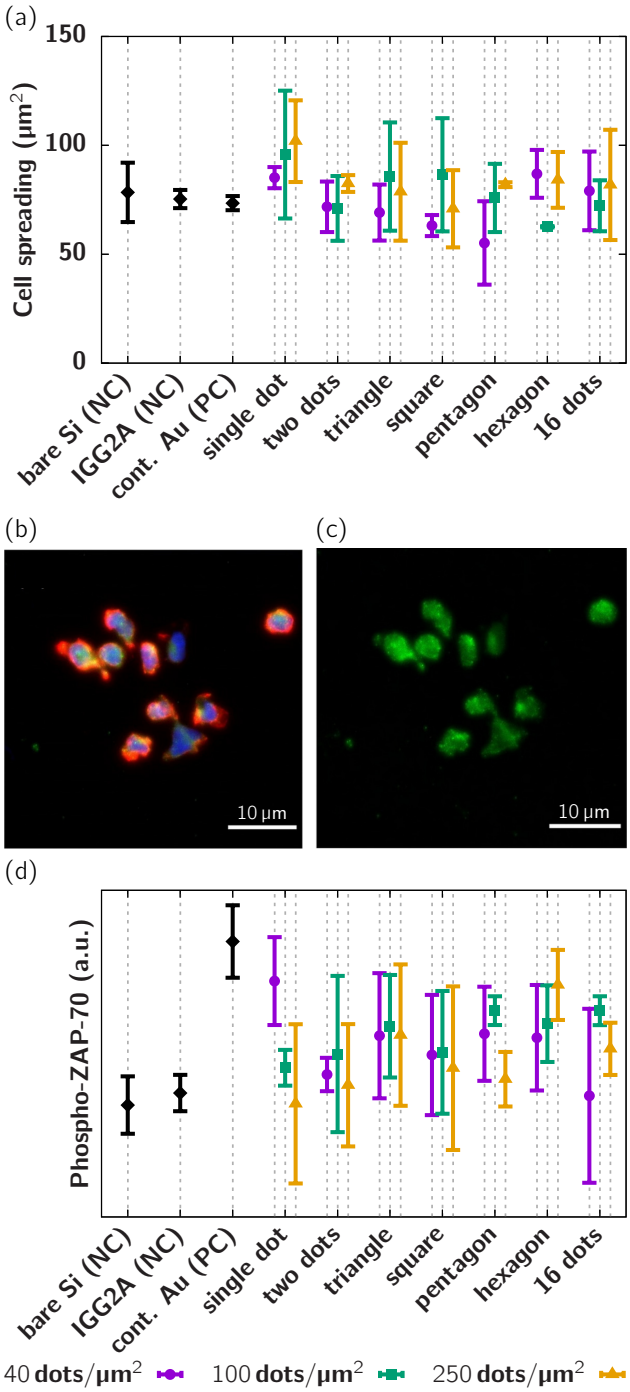

Figure 5: Characterization of natural killer activated cells. (a) Plot of the projected area of the cell cytoskeleton of cells after three hours of stimulation. (b) Confocal images of natural killer cells after showing phospho-ZAP-70 after 15 minute stimulation on nanoarrays. Cells were stained with phalloidin for cytoskeleton (red) and DAPI (blue) for nucleus and phospho-ZAP-70 (green). (c) Confocal image showing colocalization of phospho-ZAP-70. (d) Plot of overall amount of phospho-ZAP-70 after 15 minute stimulation. On graphs in panels (a) and (d) the type of pattern on the substrate (including negative controls bare Si and IGG2A, and a positive control continuous Au) is denoted on the horizontal axis.

In contrast, the mean and the variance of cell spread area are quite scattered on arrays. For a particular pattern type, typically, cells spread the most for the highest ligand density, but that trend is not systematically preserved, *e.g.*, for square patterns.

The spreading area is, furthermore, often larger for lower rather than for intermediate ligand densities. This result is consistent with the assumption that spreading itself is controlled by activation: At low ligand densities, the cells invest in spreading to increase the number of formed bonds, and potentially to activate. At intermediate densities, the sensitivity is optimal, and further spreading would not provide any additional benefit for signaling. At high densities, adhesive forces overpower active control, inducing large contact areas with the surface.

To further understand whether the ligand distribution affects early activation stages, we assessed the amount of phosphorylated ZAP-70. ZAP-70 is an early signaling cytoplasmic protein tyrosine kinase, which is recruited by activated NKG2D receptors, and whose phosphorylation is among the early stages of NKG2D signaling pathways. Here, we stimulated NK cells for 15 minutes, fixed them, and stained for fluorescently tagged phalloidin and anti-phospho-ZAP-70 (Fig. 5(b)–(c)). Finally, the overall amount of ZAP-70 is evaluated as displayed in Fig. 5(d).

We found that the ligands distribution did not produce any significant effect on the observed ZAP-70 signal. Nevertheless, for the cells stimulated on ligand arrays the observed amount of ZAP-70 is in the range of measurements for negative and positive controls. The reason underlying the indifference in ZAP-70 phosphorilation between the arrays of different densities, while the difference for CD107a was striking is not yet clearly identified. This might be because the measured amount of CD107a is cumulative, and reflects the overall amount of degranulated cells over the stimulation time. On the contrary, phosphorylation of ZAP-70, which is an early signaling event, is not cumulative. Instead, it is capturing a certain instance in time during the stimulation process (in this case, 15 minutes after the cell plating), and thus, it does not indicate the overall amount of the phosphorylation events

that happened throughout the activation. The instantaneous nature of the measurement is also consistent with large fluctuations in the data.

Finally, we checked to what extent MICA arrangement affects other NK functions, such as cytokine production. To that end, we incubated NK cells overnight on continuous arrays with various MICA densities, and tested the release of INF-γ by enzyme-linked immunosorbent assay (ELISA) of the supernatant. Contrary to CD107a, within the range of the global MICA density probed in this work, we found no effect of MICA arrangement on the release of INF-γ (Fig. S1 in SI). This difference can be explained by the fact that CD107a is a marker for lytic activity rather than cytokine secretion, and MICA–NKG2D activation of NK cells efficiently initiate the signaling pathway associated with cytotoxic granules polarization and degranulation. Other activation signals, such as those mediated by integrin molecules, are more relevant for NK cell signaling pathway associated with cytokine secretion.[46]

In summary, we have set out to deconvolve the effect of global density from the distribution of ligand–receptor bonds in the activation of NK cells using nanopatterned surfaces. In the past, nanodot arrays functionalized with anti-CD3 were used to reveal the role of antibody density and clustering in the activation of T cells.[17,19] However, due to striking differences between the antibody–receptor and ligand–receptor affinities, the antibody arrangement in these arrays did not affect T cell activation the same way the ligand arrangement does.

In contrast to those works, we here construct arrays of natural ligands permitting us to demonstrate that NK cell activation relies on biomechanical feedback: The formation of ligand–receptor bonds is producing a biochemical signal which activates the cell and increases the fluctuations of the plasma membrane. This change of state of the membrane affects the binding rates and promotes the formation of further bonds which, in turn, affects the state of the cell, until signal saturates. The experimental measurements are qualitatively explained with the postulated sigmoid relation between the average number of bonds and the membrane fluctuations. At the threshold density of $\sim$100 ligands/μm^2 this leads to a

strong dependence of cell activity on the clustering of ligands, and naturally translates to inter-cluster binding correlations.

While our membrane fluctuation model demonstrates that cells sense the average number of bonds, a natural question is if the dynamics of ligand–receptor binding and unbinding also plays a role. Correlations between bonds introduce a range of time scales in the rates, which could be exploited beyond the currently identified mechanism. Time-resolved experimental and theoretical analysis of cell activation vs. membrane activation and bond formation would be required to resolve this issue. This is an important outlook of the current work, which, as it stands, establishes a link between biomechanical feedback and biochemical signaling.

Supporting Information Available

- Details of experimental methods and theoretical model (PDF).
- Data for all the plots has been placed at Zenodo (`https://doi.org/10.5281/zenodo.11033490`).

Acknowledgement

ASS and MS gratefully acknowledge the support of German Research Foundation over the joint project SM 289/10–1. MS acknowledges the support of Israel Science Foundation, project #2016/21.

References

(1) Zhang, J.; Basher, F.; Wu, J. D. NKG2D Ligands in Tumor Immunity: Two Sides of a Coin. *Frontiers in Immunology* **2015**, *6*, 97.

(2) Shimasaki, N.; Jain, A.; Campana, D. NK cells for cancer immunotherapy. *Nature Reviews Drug Discovery* **2020**, *19*, 200–218.

(3) Xie, G.; Dong, H.; Liang, Y.; Ham, J. D.; Rizwan, R.; Chen, J. CAR-NK cells: A promising cellular immunotherapy for cancer. *eBioMedicine* **2020**, *59*, 102975.

(4) Paul, S.; Lal, G. The Molecular Mechanism of Natural Killer Cells Function and Its Importance in Cancer Immunotherapy. *Frontiers in Immunology* **2017**, *8*, 1124.

(5) Lanier, L. L. NK CELL RECOGNITION. *Annual Review of Immunology* **2005**, *23*, 225–274, PMID: 15771571.

(6) Davis, D. M.; Chiu, I.; Fassett, M.; Cohen, G. B.; Mandelboim, O.; Strominger, J. L. The human natural killer cell immune synapse. *Proceedings of the National Academy of Sciences* **1999**, *96*, 15062–15067.

(7) Orange, J. S. Formation and function of the lytic NK-cell immunological synapse. *Nature Reviews Immunology* **2008**, *8*, 713–725.

(8) Pegram, H. J.; Andrews, D. M.; Smyth, M. J.; Darcy, P. K.; Kershaw, M. H. Activating and inhibitory receptors of natural killer cells. *Immunology & Cell Biology* **2011**, *89*, 216–224.

(9) Pageon, S. V.; Cordoba, S.-P.; Owen, D. M.; Rothery, S. M.; Oszmiana, A.; Davis, D. M. Superresolution Microscopy Reveals Nanometer-Scale Reorganization of Inhibitory Natural Killer Cell Receptors upon Activation of NKG2D. *Science Signaling* **2013**, *6*, ra62–ra62.

(10) van der Merwe, P. A.; Dushek, O. Mechanisms for T cell receptor triggering. *Nature Reviews Immunology* **2011**, *11*, 47–55.

(11) Kumar, S. Natural killer cell cytotoxicity and its regulation by inhibitory receptors. *Immunology* **2018**, *154*, 383–393.

(12) Mbiribindi, B.; Mukherjee, S.; Wellington, D.; Das, J.; Khakoo, S. I. Spatial Clustering of Receptors and Signaling Molecules Regulates NK Cell Response to Peptide Repertoire Changes. *Frontiers in Immunology* **2019**, *10*.

(13) Goyette, J.; Nieves, D. J.; Ma, Y.; Gaus, K. How does T cell receptor clustering impact on signal transduction? *Journal of Cell Science* **2019**, *132*, jcs226423.

(14) Davis, S. J.; van der Merwe, P. A. The kinetic-segregation model: TCR triggering and beyond. *Nature Immunology* **2006**, *7*, 803–809.

(15) Li, L.; Stumpf, B. H.; Smith, A.-S. Molecular Biomechanics Controls Protein Mixing and Segregation in Adherent Membranes. *International Journal of Molecular Sciences* **2021**, *22*, 3699.

(16) Dushek, O.; Goyette, J.; van der Merwe, P. A. Non-catalytic tyrosine-phosphorylated receptors. *Immunological Reviews* **2012**, *250*, 258–276.

(17) Matic, J.; Deeg, J.; Scheffold, A.; Goldstein, I.; Spatz, J. P. Fine Tuning and Efficient T Cell Activation with Stimulatory aCD3 Nanoarrays. *Nano Letters* **2013**, *13*, 5090–5097.

(18) Deeg, J.; Axmann, M.; Matic, J.; Liapis, A.; Depoil, D.; Afrose, J.; Curado, S.; Dustin, M. L.; Spatz, J. P. T Cell Activation is Determined by the Number of Presented Antigens. *Nano Letters* **2013**, *13*, 5619–5626.

(19) Cai, H.; Muller, J.; Depoil, D.; Mayya, V.; Sheetz, M. P.; Dustin, M. L.; Wind, S. J. Full control of ligand positioning reveals spatial thresholds for T cell receptor triggering. *Nature Nanotechnology* **2018**, *13*, 610–617.

(20) Cai, H.; Wolfenson, H.; Depoil, D.; Dustin, M. L.; Sheetz, M. P.; Wind, S. J. Molecular Occupancy of Nanodot Arrays. *ACS Nano* **2016**, *10*, 4173–4183.

(21) Keydar, Y.; Le Saux, G.; Pandey, A.; Avishay, E.; Bar-Hanin, N.; Esti, T.; Bhingardive, V.; Hadad, U.; Porgador, A.; Schvartzman, M. Natural killer cells' immune

response requires a minimal nanoscale distribution of activating antigens. *Nanoscale* **2018**, *10*, 14651–14659.

(22) Toledo, E.; Saux, G. L.; Edri, A.; Li, L.; Rosenberg, M.; Keidar, Y.; Bhingardive, V.; Radinsky, O.; Hadad, U.; Primo, C. D.; Buffeteau, T.; Smith, A.-S.; Porgador, A.; Schvartzman, M. Molecular-scale spatio-chemical control of the activating-inhibitory signal integration in NK cells. *Sci. Adv.* **2021**, *7*, eabc1640.

(23) Monzel, C.; Schmidt, D.; Kleusch, C.; Kirchenbüchler, D.; Seifert, U.; Smith, A.-S.; Sengupta, K.; Merkel, R. Measuring fast stochastic displacements of bio-membranes with dynamic optical displacement spectroscopy. *Nat. Commun.* **2015**, *6*, 8162.

(24) Turlier, H.; Fedosov, D. A.; Audoly, B.; Auth, T.; Gov, N. S.; Sykes, C.; Joanny, J.-F.; Gompper, G.; Betz, T. Equilibrium physics breakdown reveals the active nature of red blood cell flickering. *Nat. Phys.* **2016**, *12*, 513–519.

(25) Brodovitch, A.; Limozin, L.; Bongrand, P.; Pierres, A. Use of TIRF to Monitor T-Lymphocyte Membrane Dynamics with Submicrometer and Subsecond Resolution. *Cellular and Molecular Bioengineering* **2015**, *8*, 178–186.

(26) Biswas, A.; Alex, A.; Sinha, B. Mapping Cell Membrane Fluctuations Reveals Their Active Regulation and Transient Heterogeneities. *Biophysical Journal* **2017**, *113*, 1768–1781.

(27) Turlier, H.; Betz, T. Unveiling the Active Nature of Living-Membrane Fluctuations and Mechanics. *Annual Review of Condensed Matter Physics* **2019**, *10*, 213–232.

(28) Begemann, I.; Saha, T.; Lamparter, L.; Rathmann, I.; Grill, D.; Golbach, L.; Rasch, C.; Keller, U.; Trappmann, B.; Matis, M.; Gerke, V.; Klingauf, J.; Galic, M. Mechanochemical self-organization determines search pattern in migratory cells. *Nature Physics* **2019**, *15*, 848–857.

(29) Santoni, G.; Amantini, C.; Santoni, M.; Maggi, F.; Morelli, M. B.; Santoni, A. Mechanosensation and Mechanotransduction in Natural Killer Cells. *Frontiers in Immunology* **2021**, *12*, 688918.

(30) Ben-Shmuel, A.; Sabag, B.; Biber, G.; Barda-Saad, M. The Role of the Cytoskeleton in Regulating the Natural Killer Cell Immune Response in Health and Disease: From Signaling Dynamics to Function. *Frontiers in Cell and Developmental Biology* **2021**, *9*, 609532.

(31) Olofsson, P. E.; Forslund, E.; Vanherberghen, B.; Chechet, K.; Mickelin, O.; Rivera Ahlin, A.; Everhorn, T.; Önfelt, B. Distinct Migration and Contact Dynamics of Resting and IL-2-Activated Human Natural Killer Cells. *Frontiers in Immunology* **2014**, *5*, 80.

(32) Zhu, Y.; Xie, J.; Shi, J. Rac1/ROCK-driven membrane dynamics promote natural killer cell cytotoxicity via granzyme-induced necroptosis. *BMC Biology* **2021**, *19*, 140.

(33) Bihr, T.; Seifert, U.; Smith, A.-S. c. v. Nucleation of Ligand-Receptor Domains in Membrane Adhesion. *Phys. Rev. Lett.* **2012**, *109*, 258101.

(34) Fenz, S. F.; Bihr, T.; Schmidt, D.; Merkel, R.; Seifert, U.; Sengupta, K.; Smith, A.-S. Membrane fluctuations mediate lateral interaction between cadherin bonds. *Nat. Phys.* **2017**, *13*, 906–913.

(35) Valitutti, S.; Müller, S.; Cella, M.; Padovan, E.; Lanzavecchia, A. Serial triggering of many T-cell receptors by a few peptide–MHC complexes. *Nature* **1995**, *375*, 148–151.

(36) Janeš, J. A.; Monzel, C.; Schmidt, D.; Merkel, R.; Seifert, U.; Sengupta, K.; Smith, A.-S. First-Principle Coarse-Graining Framework for Scale-Free Bell-Like Association and Dissociation Rates in Thermal and Active Systems. *Phys. Rev. X* **2022**, *12*, 031030.

(37) Wu, X.; Sharma, A.; Oldenburg, J.; Weiher, H.; Essler, M.; Skowasch, D.; Schmidt-Wolf, I. G. H. NKG2D Engagement Alone Is Sufficient to Activate Cytokine-Induced Killer Cells While 2B4 Only Provides Limited Coactivation. *Frontiers in Immunology* **2021**, *12*, 731767.

(38) Urlaub, D.; Höfer, K.; Müller, M.-L.; Watzl, C. LFA-1 Activation in NK Cells and Their Subsets: Influence of Receptors, Maturation, and Cytokine Stimulation. *The Journal of Immunology* **2017**, *198*, 1944–1951.

(39) Arnold, M.; Cavalcanti-Adam, E. A.; Glass, R.; Blümmel, J.; Eck, W.; Kantlehner, M.; Kessler, H.; Spatz, J. P. Activation of Integrin Function by Nanopatterned Adhesive Interfaces. *ChemPhysChem* **2004**, *5*, 383–388.

(40) Schvartzman, M.; Palma, M.; Sable, J.; Abramson, J.; Hu, X.; Sheetz, M. P.; Wind, S. J. Nanolithographic Control of the Spatial Organization of Cellular Adhesion Receptors at the Single-Molecule Level. *Nano Letters* **2011**, *11*, 1306–1312.

(41) Bauer, S.; Groh, V.; Wu, J.; Steinle, A.; Phillips, J. H.; Lanier, L. L.; Spies, T. Activation of NK Cells and T Cells by NKG2D, a Receptor for Stress-Inducible MICA. *Science* **1999**, *285*, 727–729.

(42) Le Saux, G.; Edri, A.; Keydar, Y.; Hadad, U.; Porgador, A.; Schvartzman, M. Spatial and Chemical Surface Guidance of NK Cell Cytotoxic Activity. *ACS Applied Materials & Interfaces* **2018**, *10*, 11486–11494.

(43) Bálint, Š.; Lopes, F. B.; Davis, D. M. A nanoscale reorganization of the IL-15 receptor is triggered by NKG2D in a ligand-dependent manner. *Science Signaling* **2018**, *11*, eaal3606.

(44) Alter, G.; Malenfant, J. M.; Altfeld, M. CD107a as a functional marker for the identification of natural killer cell activity. *Journal of Immunological Methods* **2004**, *294*, 15–22.

(45) Schmidt, D.; Bihr, T.; Seifert, U.; Smith, A.-S. Coexistence of dilute and densely packed domains of ligand-receptor bonds in membrane adhesion. *Europhys. Lett.* **2012**, *99*, 38003.

(46) Perussia, B. Signaling for cytotoxicity. *Nature Immunology* **2000**, *1*, 372–374.